CHAPTER III

THEORY

3.1 Molecular Sieves for Use in Catalysis

3.1.1 Structure Overview

Zeolites and molecular sieves are finding applications in many areas of catalysis, generating interest in these materials in industrial and academic laboratories. As catalyst, zeolites exhibit appreciable acid activity with shape-selectivity features not available in the compositional equivalent amorphous catalysts. In addition, these materials can act as supports for numerous catalytically active metals. Major advances have occurred in the synthesis of molecular sieve materials since the initial discovery of the synthetic zeolite molecular sieve's type A, X and Y, and a great number of techniques have evolved for identifying and characterizing these materials. Added to and extensive and ever growing list of aluminosilicate zeolites are molecular sieves containing other elemental compositions. These materials differ in their catalytic activity relative to the aluminosilicate zeolites and may have potential in customizing or tailoring the molecular sieves catalyst for specific applications. Elements isoeletronic with Al^{+3} or Si^{+4} have been proposed to substitute into the framework lattice during synthesis. These include B^{+3}, Ga^{+3}, Fe^{+3}, and Cr^{+3} substituting for Al^{+3}, and Ge^{+4} and Ti^{+4} for Si^{+4}. The incorporation of transition elements such as Fe^{+3} for framework Al^{+3} positions modifies the acid activity and, in addition, provides a novel means of obtaining high dispersions of these metals within the constrained pores of industrially interesting catalyst materials.

Another class of materials shown to crystallize into molecular sieve structures are the aluminophosphate($AlPO_4$) molecular sieves. Structural analogs to the zeolites as well as new structures have been prepared with this elemental composition, including one with a

pore size greater than that of faujasite. Unlike the zeolites, these materials have no ion exchange capacity, as they possess a balanced framework charge. Through modification of synthesis conditions, silicon has been incorporated into many of the $AlPO_4$ structures. Addition of structural silicon enhances both hydrophilicity and catalytic acid activity, and ion exchange capacity is imparted. Other ions such as magnesium, zinc, cobalt, and manganese also may occupy sites in the $AlPO_4$ framework. These materials are expected to contain different charged sites within the structure, potentially providing further alteration (tailoring) of catalytic behavior.

The possibilities for new zeolite structures and new molecular sieve materials appear limited only by the abilities of those skilled in synthesis to develop methods for their preparation and of the physical scientist to identify and characterize their structures and properties.

3.1.2 Molecular sieve vs. zeolite: A Definition

With the recent discoveries of molecular sieve materials containing other elements in addition to, or in lieu of , silicon and aluminum, the casual interchange of the terms" molecular sieve " and "zeolite " must be reconsidered. In 1932 McBain proposed the " molecular sieve " to describe a class of materials that exhibited selective adsorption properties. He proposed that for a material to be a molecular sieves , it must separate components of mixture on the basis of molecular size and shape differences. Two classes of molecular sieves were known when McBain put forth his definition: the zeolites and certain microporous charcoals. The list now includes the silicates, the metallosilicates, metalloaluminates, the $AlPO_4$s, and silico-and metalloaluminophosphates, as well as the zeolites. The different classes of molecular sieve materials are listed in figure 3.1 . All are molecular sieves, as their regular framework structures will separate components of a mixture on the basis of size and shape. The difference lies not within the structure of a

mixture these materials, as many are structurally analogous, but in their elemental composition. Therefore, all are molecular sieves though none but the aluminosilicates should carry the classical name, zeolite [66].
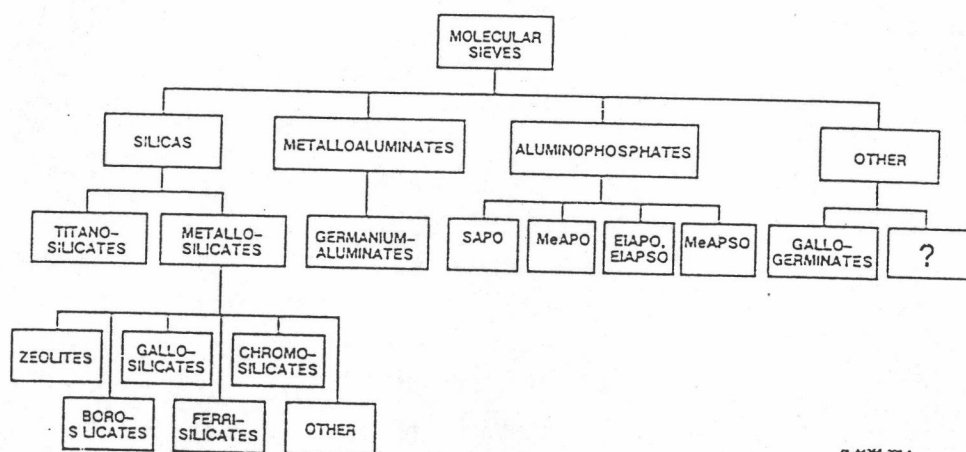

Figure 3.1 Classification of molecular sieve materials indicating extensive variation in composition. The zeolites occupy a subcategory of the metallosilicates [66].

3.1.3 Structure of Zeolite

Zeolite are pore, crystalline aluminosilicates that develop uniform pore structure having minimum channel diameter of 0.3-0.1 nm. This size depends primarily upon the type of zeolite.

Zeolite provide high activity and unusual selectivity in a variety of acid-catalyzed reactions. Most of the reaction are caused by the acidic nature of zeolites.

The structure of zeolite consists of a three - dimensional framework of SiO_4 or AlO_4 tetrahedra, each of which contains a silicon or aluminum atom in the center. The oxygen atoms are shared between adjoining tetrahedra, which can be present in various ratios and arranged in a variety of way. The framework thus obtained contains pores, channels, and cages, or interconnected voids.

Zeolites may be represent by the general formular,

$$M_{x/n}[(AlO_4)_x(SiO_2)_y]wH_2O$$
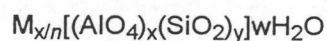
where the term in brackets is the crystallographic unit cell. The metal cation of valence n is present to produce electrical neutrality since for each aluminum tetrahedron in the lattice there is an overall charge of -1 [67]. M is a proton, the zeolite becomes a strong Bronsted acid. As catalyst , zeolite becomes a strong Bronsted acid. As catalysts, zeolites are unique in their ability to discriminate between reactant molecular size and shape [68].

The catalytically most significant are those having pore openings characterized by 8-, 10- , and 12- rings of oxygen atoms. Some typical pore geometries are shown in figure 3.2 [69].

The framework of zeolites used most frequently as adsorbent or catalyst are shown in figure 3.3 -3.6. The Al or Si atoms are located at the intersection of lines that represent oxygen bridges. The X and Y zeolites are structurally and topologically related to the mineral faujasite and frequently refereed to as faujasite-type zeolites. The two materials differ chemically by their Si/Al ratios, which are 1-1.5 and 1.5-3.0 for X and Y zeolite,

respectively. In faujasites, large cavities of 1.3 nm in diameter (supercages) are connected to each other through apertures of 1.0 nm.
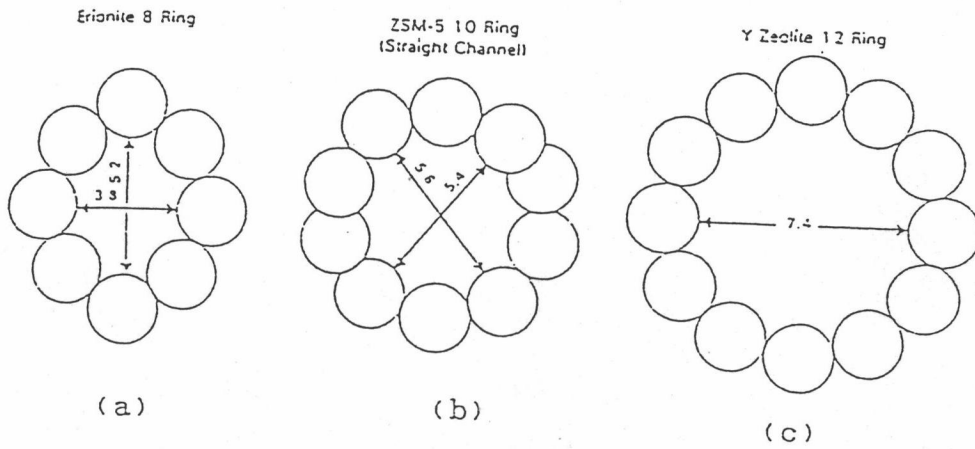

(a)   (b)   (c)

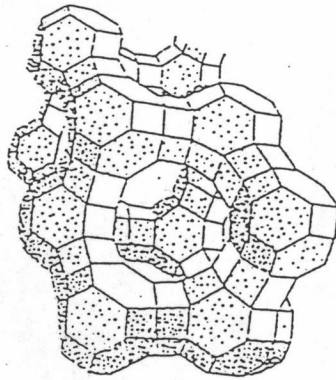Figure 3.2 Typical zeolite pore geometries [69].

Figure 3.3 Structure of type-Y(or X) zeolite [67].
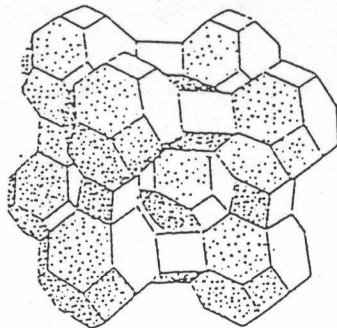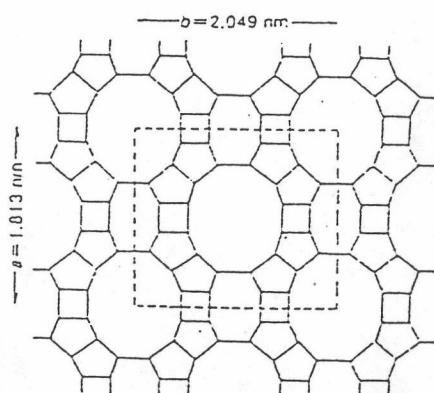

Figure 3.4 Structure of type-A zeolite [67].

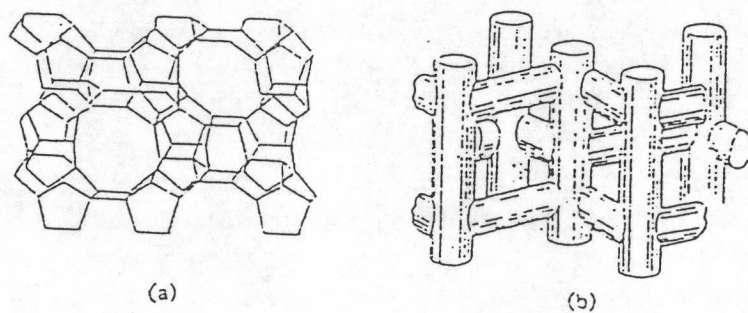Figure 3.5 Skeletal diagram of the (001) face of mordenite [67].

(a)

(b)

Figure 3.6 Structure of ZSM-5 (a) Skeletal diagram of the (010)

face of ZSM-5 (b) channel network [67].

In type A zeolite (figure 3.4) , large cavities are connected through apertures of 0.5 nm, determined by eight-member rings (figure 3.2 a)

The mordenite pore structure (figure 3.5) consists of elliptical and non interconnected channels parallel to the c-axis of the orthorhombic structure. Their openings are limited by twelve-member rings(0.6-0.7 nm) (figure 3.2 c). ZSM-5 zeolite (figure 3.6) shows a unique pore structure that consists of two intersection channel systems: one straight and the other sinusoidal and perpendicular to the former (figure 3.6). Both channel systems have ten-member-rings elliptical openings (ca. 0.55 A in diameter) (figure 3.2 b).

3.2 Acidity of Zeolite

Classical Bronsted and Lewis acid models of acidity have been used to classify the active sites on zeolites. Bronsted acidity is proton donor acidity; a trigonally co-ordinated alumina atom is an electron deficient and can accept an electron pair, therefore behaves as a Lewis acid [68, 70].

In general, the increase in Si/Al ratio will increase acidic strength and thermal stability of zeolite [71]. Since the number of acidic OH groups depend on the number of aluminum in zeolite's framework, decrease in Al content is expected to reduce catalytic activity of zeolite. If the effect of increase in the acidic centers, decrease in Al content shall result in enhancement of catalytic activity.

Based on electrostatic consideration, the charge density at a cation site increases with increasing Si/Al ratio. It was conceived that these phenomena are related to reduction

of electrostatic interaction between framework sites, and possibly to difference in the order of aluminum in zeolite crystal-the location of Al in crystal structure [70].

Recently it has been reported the mean charge on the proton was shifted regularly towards higher values as the Al content decreased [68]. Simultaneously the total number of acidic hydroxyls, governed by the Al atoms, were decreases. This evidence emphasized that the entire acid strength distribution(weak, medium, strong) was shifted towards stronger values. That is, weaker acid sites become stronger with the decrease in Al content.

An improvement in thermal or hydrothermal stability has been ascribed to the lower density of hydroxyls groups which parallel to that of Al content [67]. A longer distance between hydroxyl groups decreases the probability of dehydroxylation that generates defects on structure of zeolites.

3.3 Generation of Acid Centers

Protonic acid centers of zeolite are generated invarious ways. Figure 3.7 depicts the thermal decomposition of ammonium exchanged zeolites yielding the hydrogen form [66].

The Bronsted acidity due to water ionization on polyvalent cations, described below, is depicted in figure 3.8 [67].

$$M^{n+} + xH_2O \longrightarrow M(OH)_x^{(n-x)+} + xH^+ \qquad (3.1)$$
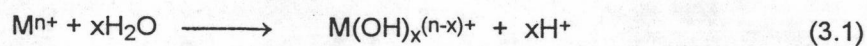
The exchange of monovalent ions by polyvalent cations could improve the catalytic property. Those highly charged cations create very acidic centers by hydrolysis phenomena.

Bronsted acid sites are also generated by the reduction of transition metal cations. The concentration of OH groups of zeolite containing transition metals was noted to

increase by reduction with hydrogen at 250-450 $^{\circ}$C at to increase with the rise of the reduction temperature [1].

$$Cu^{2+} + H_2 \longrightarrow Cu^0 + 2H^+ \qquad (3.2)$$

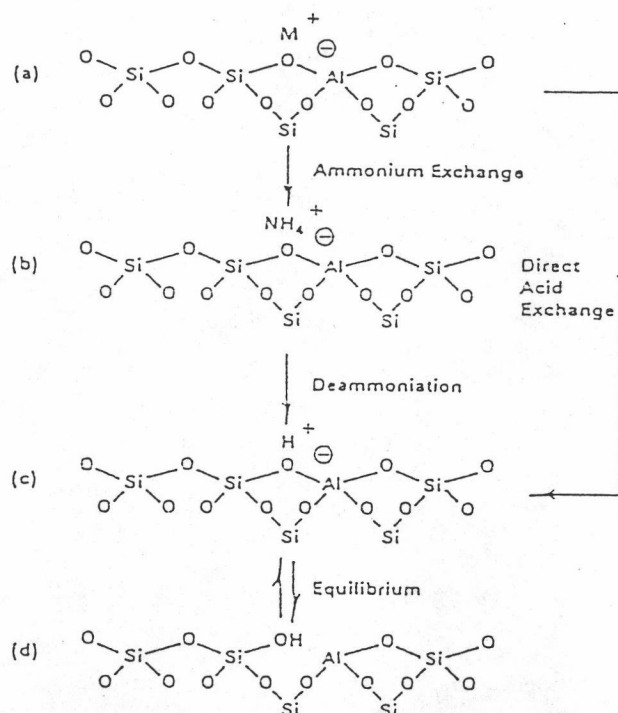$$Ag^+ + 1/2H_2 \longrightarrow Ag^0 + H^+ \qquad (3.3)$$

Figure 3.7 Diagram of the surface of a zeolite framework [66].

a) In the as-synthesized from M^+ is either an organic cation or an alkalimetal cation.

b) Ammonium in exchange produces the NH_4^+ exchanged form.

c) Thermal treatment is used to remove ammonia, producing the H^+ , acid, form.

d) The acid form in (c)is in equilibrium with the form shown in (d), where there is a silanol group adjacent to a tricoordinate aluminum.
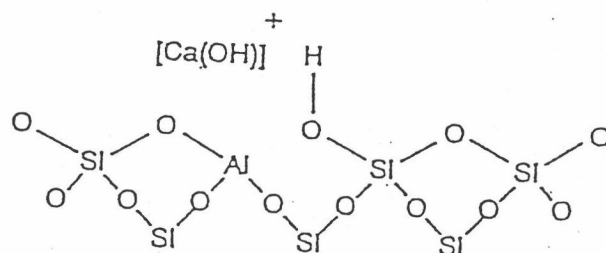
Figure 3.8 Water molecules coordinated to polyvalent cation are dissociated by

heat treatment yielding Bronsted acidity [67].

The formation of Lewis acidity from Bronsted sites is depicted in figure 3.9 [67]. The dehydration reaction decreases the number of protons and increases that of Lewis sites.

Bronsted(OH) and Liwis(-Al-) sites can be present simultaneously in the structure of zeolite at high temperature. Dehydroxylation is thought to occur in ZSM-5 zeolite above 500 °C and calcination at 800 to 900 °C produces irreversible dehydroxylation which causes defection in crystal structure of zeolite.

Dealumination is believed to occur during dehydroxylation which may result from the steam generation within the sample. The dealumination is indicated by an increase in the surface concentration of aluminum on the crystal. The dealumination process is expressed in Figure 3.9. The extent of dealumination monotonously increases with the partial pressure of steam.

The enhancement of the acid strength of OH groups is recently proposed to be pertinent to their interaction with those aluminum species sites are tentatively expressed in figure 3.10 [67]. Partial dealumination might, therefore, yield a catalyst of higher activity while severe steaming reduces the catalytic activity.
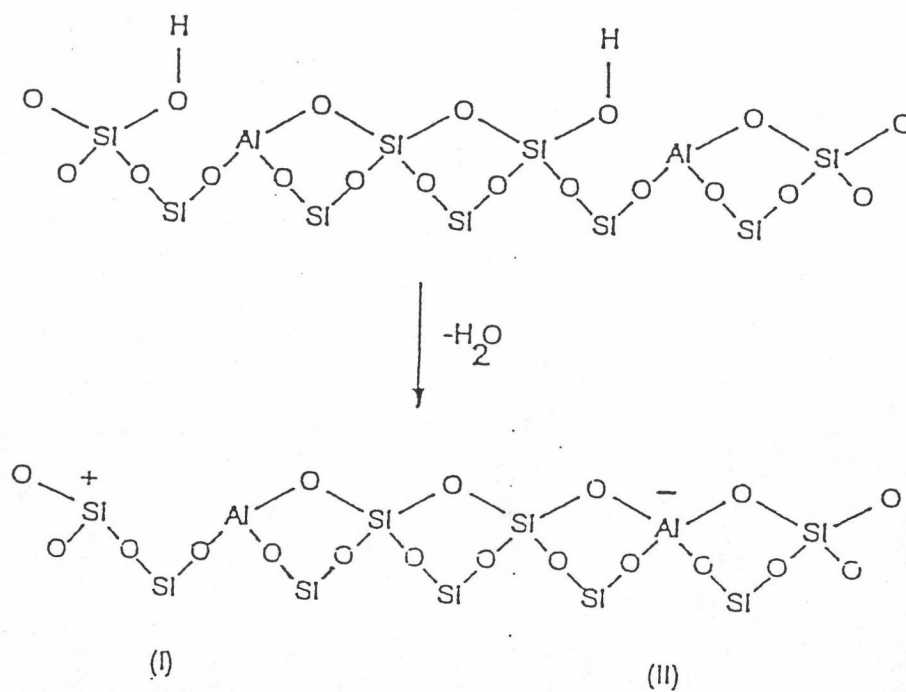
Figure 3.9 Lewis acid site developed by dehydroxylation of Bronsted acid site [67].
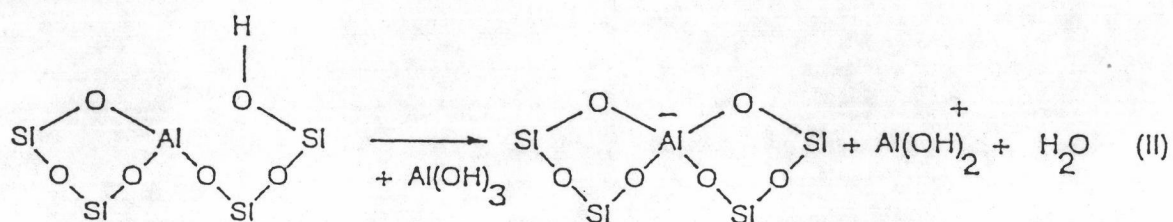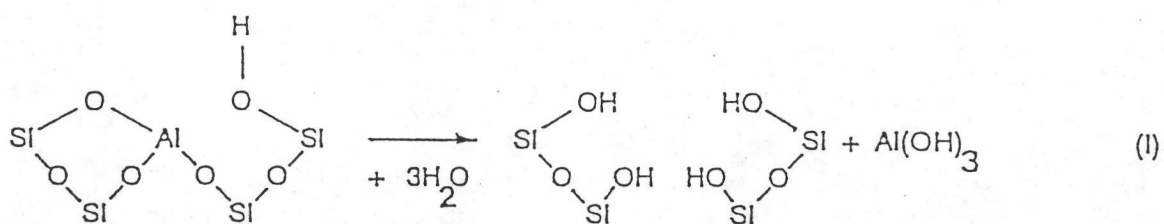

Figure 3.10 Steam dealumination process in zeolite [67].
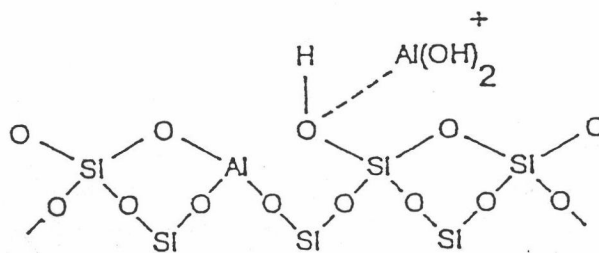
Figure 3.11 The enhancement of the acid strength of OH groups by their interaction
with dislodged aluminum species [67].

3.4 Shape Selectivity

Many reactions involving carbonium ions intermediates are catalyzed by acidic zeolites. With respect to a chemical standpoint the reaction mechanisms are not fundamentally different with zeolites or with any other acidic oxides. What zeolite add is shape selectivity effect. The shape selective characteristics of zeolites influence their catalytic phenomena by three modes; reactants shape selectivity, products shape selectivity and transition states shape selectivity [72-73]. These type of selectivity are depicted in figure 3.12 [66].

Reactant or charge selectivity results from the limited diffusibility of some of reactants, which cannot effectively enter and diffuse inside crystal pore structures of the zeolites.

Product shape selectivity occurs as slowly diffusing product molecules cannot escape from the crystal and undergo secondary reactions.

a) Reactant selectivity
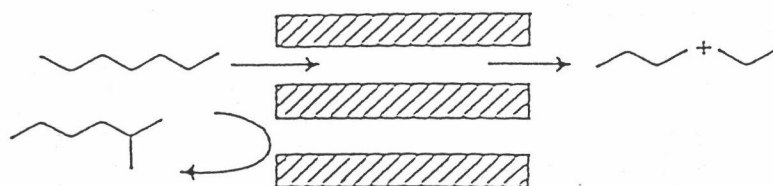
b) Product selectivity
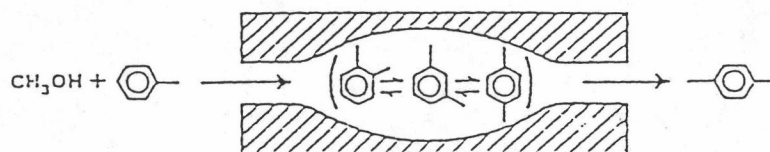
c) Transient state selectivity
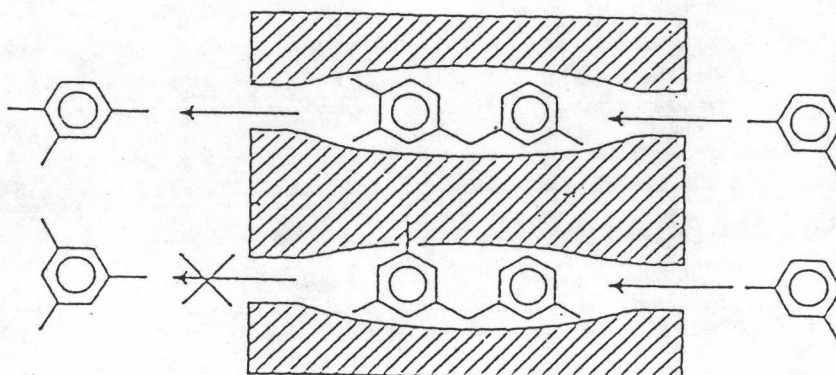
Figure 3.12 Diagram depicting the three type of selectivity [66].

Table 3.1 Kinetic diameters of various molecules based on the Lenard-Jones relationship
[74].

	KINETIC DIAMETER (ANGSTROMS)
He	2.6
H_2	2.89
O_2	3.46
N_2	3.64
NO	3.17
CO	3.76
CO_2	3.3
H_2O	2.65
NH_3	2.6
CH_4	3.8
C_2H_2	3.3
C_2H_4	3.9
C_3H_8	4.3
$n-C_4H_{10}$	4.3
Cyclopropane	4.23
$i-C_4H_{10}$	5.0
$n-C_5H_{12}$	4.9
SF_6	5.5
Neopentane	6.2
$(C_4F_9)_3N$	10.2
Benzene	5.85
Cyclohexane	6.0
m-xylene	7.1
p-xylene	6.75
1,3,5 trimethylbenzene	8.5
1,3,5 triethylbenzene	9.2
1,3 diethylbenzene	7.4
1-methylnaphthalene	7.9
$(C_4H_9)_3N$	8.1

This reaction path is established by monitoring changes in product distribution as a function
of varying contact time.

Table 3.2 Shape of the pore mouth opening of known zeolite structures. The dimensions are based on two parameters, the T atom forming the channel opening (8, 10, 12 rings) and the crystallographic free diameters of the channels. The channels are parallel to the crystallographic axis shown in brackets (e.g. <100>) [66].

STRUCTURE	8-MEMBER RING	10-MEMBER RING	12-MEMBER RING
Bikitaite	3.2 × 4.9 [001]		
Brewsterite	2.3 × 5.0 [100]		
	2.7 × 4.1 [001]		
Cancrinite			6.2 [001]
Chabazite	3.6 × 3.7 [001]		
Dachiardite	3.6 × 4.8 [001]	3.7 × 6.7 [010]	
TMA-E	3.7 × 4.8 [001]		
Edingtonite	3.5 × 3.9 [110]		
Epistilbite	3.7 × 4.4 [001]	3.2 × 5.3 [100]	
Erionite	3.6 × 5.2 [001]		
Faujasite			7.4 <111>
Ferrierite	3.4 × 4.8 [010]	4.3 × 5.5 [001]	
Gismondine	3.1 × 4.4 [100]		
	2.8 × 4.9 [010]		
Gmelinite	3.6 × 3.9 [001]		7.0 [001]
Heulandite	4.0 × 5.5 [100]	4.4 × 7.2 [001]	
	4.1 × 4.7 [001]		
ZK-5	3.9 <100>		
Laumontite		4.0 × 5.6 [100]	
Levyne	3.3 × 5.3 [001]		
Type A	4.1 <100>		
Type L			7.1 [001]
Mazzite			7.4 [001]
ZSM-11		5.1 × 5.5 [100]	
Merlinoite	3.1 × 3.5 [100]		
	3.5 × 3.5 [010]		
	3.4 × 5.1 [001]		
	3.3 × 3.3 [001]		
ZSM-5		5.4 × 5.6 [010]	
		5.1 × 5.5 [100]	
Mordenite	2.9 × 5.7 [010]		6.7 × 7.0 [001]
Natrolite	2.6 × 3.9 <101>		
Offretite	3.6 × 5.2 [001]		6.4 [001]
Paulingite	3.9 <100>		
Phillipsite	4.2 × 4.4 [100]		
	2.8 × 4.8 [010]		
	3.3 [001]		
Rho	3.9 × 5.1 <100>		
Stilbite	2.7 × 5.7 [101]	4.1 × 6.2 [100]	
Thomsonite	2.6 × 3.9 [101]		
	2.6 × 3.9 [010]		
Yugawaralite	3.1 × 3.5 [100]		
	3.2 × 3.3 [001]		
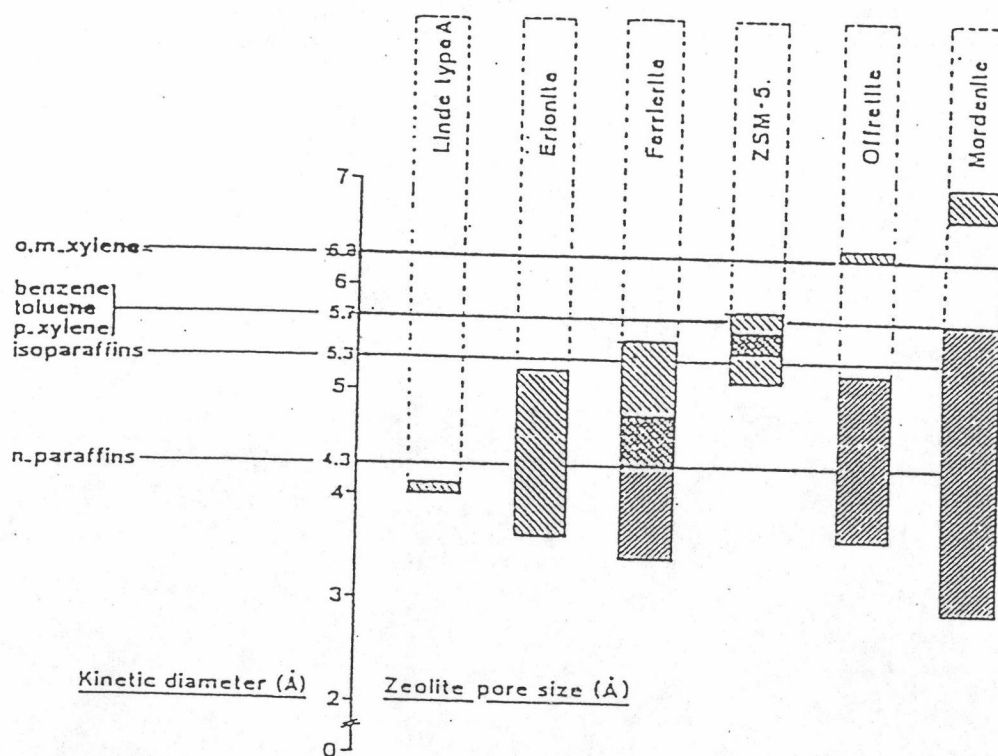
Figure 3.13 Correlation between pore size(s) of various zeolites and kinetic

diameter of some molecules [72].

Restricted transition state shape selectivity is a kinetic effect arising from local environment around the active site, the rate constant for a certain reaction mechanism is reduced if the space required for formation of necessary transition state is restricted.

The critical diameter (as opposed to the length) of the molecules and the pore channel diameter of zeolites are important in predicting shape selective effects. However, molecules are deformable and can pass through openings which are smaller than their critical diameters. Hence, not only size but also the dynamics and structure of the molecules must be taken into account.

Table 3.1 [9] presents values of selected critical molecular diameters and Table 3.2 [66] presents values of the effective pore size of various zeolites. Correlation between pore size(s) of zeolites and kinetic diameter of some molecules are depicted in figure 3.13 [72].

3.5 Non - aluminosilicate Molecular Sieves

Advances in the area of new molecular sieve materials have come in the preparation of zeolite - like structure containing framework components other than aluminum and silicon exclusively. The aluminosilicate zeolites offer the ion exchange properties, higher thermal stability, high acidity and shape - selective structural features desired by those working in the areas of adsorption and catalysis. However, modification and subsequent improvement of these properties have served as a driving force for changing the composition of these microporous materials.

It is well accepted that gallium can easily be substituted for aluminum and germanium for silicon in aluminosilicate system, as these elements are in the same family of the periodic table. Gallosilicate, gallogerminate and germanium aluminate analogs of the known zeolites have been hydrothermally synthesized under conditions comparable to the zeolite molecular sieves. Other elements were found not to substitute so easily. In the crystallization of many zeolite structures, the relative amounts of silicon and aluminum in the reacting gel strongly influenced the crystallization of a particular structure. Attempts to substitute vastly different elements for either aluminum or silicon resulted in suppression of crystallization. It was the discovery of the strong structure - directing properties of the cation organic amine additives that fuelled new discoveries of different chemical compositions with zeolite - like structures. The graph in figure 3.14 [66] show this explosion in new (non-zeolitic) molecular sieves patented relative to the reported new zeolite materials synthesized and the nature zeolite mineral known. The number of non-zeolite molecular sieves reported

is far greater than the number of microporous aluminosilicate zeolite materials as shown in the graph.

In addition to the gallosilicates, germanium aluminates, and galleminates synthesized prior to the use of organic additives, materials containing zeolite - type structures crystallized in the presence of organic cation have been claimed to contain boron, iron, chromium, cobalt, titanium, zirconium, zinc, beryllium, hafnium, manganese, magnesium, vanadium, and tin. Little characterization of the extent of incorporation has been presented for many of these materials. The most common structure claims to in corporate such elements is the ZSM-5 type framework.

However, it is well accepted that the ZSM-5 structure, strongly directed by the presence of the TPA cation, can easily crystallize in the pure silica form (silicate). Therefore, the possibility remain , without sufficient characterization to confirm incorporation, that this exclusively silica-containing structure could form metallosilicate reaction reaction mixture, giving the characteristic X-ray diffraction pattern without incorporating the desired metal component into the structure. Boron, gallium, iron, and titanium have been sufficiently characterized to confirm structure incorporation.

Figure 3.14 A comparison of the natural zeolites known and the number of zeolites synthesized within the last 30 years with the number of recently patented non-zeolite molecular sieves [66].

3.6 Acidity of Metallosicate

The synthesis of zeolites containing various elements such as B, P, or Ge has been carried out for a long time. Since the discovery of ZSM-5 (aluminosilicate) and silicalite, many attempts have been made to synthesize the metallosicilicate with the ZSM-5 structure. The isomorphous substitution of aluminum with other elements greatly modifies the acidic properties of the silicate. The elements introduced include, Be, B, Ti, Cr, Fe, Zn, Ga, and V. These elements were usually introduced by adding metal salts as one of the starting materials for the synthesis of the metallosilicate. It is also known that boron can be directly introduced by reacting ZSM-5 with boron trichloride. Metallosilicate with a ZSM-5 structure having metal M as a component will be denoted [M]-ZSM-5, hereafter. Silicate II (the framework topology of which is structurally identical to that of ZSM-11) can be transformed into gallosilicate with its reaction with $NaGaO_2$ in an aqueous solution.
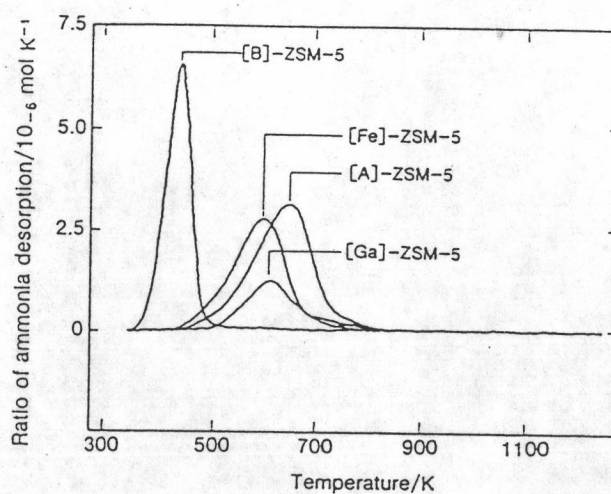

Figure 3.15 Temperature programmed desorption of ammonia from metallosilicate (Reported with permission by C. T - W. Chu, C. D. Chang, J. Phys, Chem., 89, 1571(1985)) [67].

Figure 3.15 [67] shows the TPD spectrum of ammonia adsorbed on various metallosilicate. The acid strength of metallosilicate changes in decreasing order as follows:

[Al] - ZSM-5 > [Ga] - ZSM-5 > [Fe] - ZSM-5 >[B] - ZSM-5

The band position of OH groups changes in conformity with TPD spectra. Thus, the OH band appears at 3610, 3620, 3630, and 3725 cm^{-1} for [Al]-, [Ga]-, [Fe]-, and [B]-ZSM-5, respectively. The fact that the acid strength of [B]-ZSM-5 is much weaker than that of [Al]-ZSM-5 has been reported by several authors.

Table 3.3   Product distribution of the conversion of 1-butene over H-ZSM-5,

H-[B]-ZSM-5 and Zn-[B]-ZSM-5 [67].

| Catalyst	H-[Al]-ZSM-5	H-[B]-ZSM-5	Zn-[B]-ZSM-5
conversion/%	77.3	71.7	81.2
Products/%[t1]			
$C_1 \sim C_4$ alkanes	41.3	5.1	6.3
$C_2H_4 + C_3H_6$	14.6	38.3	21.1
C_4H_8[t2]	6.2	28.3	27.7
C_5^+	2.4	25.3	7.0
aromatics	37.0	3.0	38.0

Reaction conditions, 773 K, W/F=5.3 g h mol^{-1}
1-butene=23.0 kPa
[t1] carbon-number basis,   [t2] including 1-butene

Weaker acid strength of [B]-ZSM-5 is confirmed also by catalytic reactions. Table 3.3 [67] shows the product distributions of 1-butene reaction over [B]-ZSM-5 and [A]-ZSM-5 at 773 K. It is clear that there is a great difference in the product dismatic hydrocarbons, while over [B]-

ZSM-5, lower alkenes are the main products. This indicates that the hydride transfer reactions from alkene to carbonium ion does not proceed over [B]-ZSM-5.

R+   RH (alkane)   alkanes

$\longrightarrow$ + $\longrightarrow$

C-C=C-C-C-C   C-C=C=C-C-C   aromatics
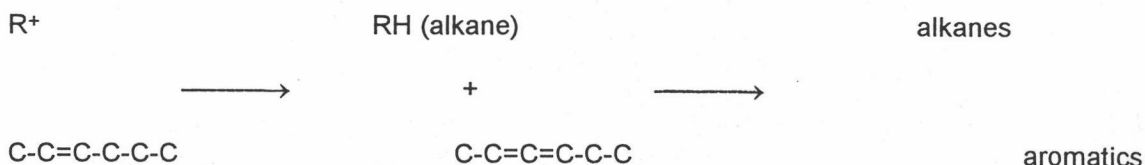
For the same reasons, alkenes are the main products in the conversion of methanol over [B]-ZSM-5, while [Al]-ZSM-5   is a unique catalyst for gasoline production.

The yield of aromatic hydrocarbons greatly increases by introducing zinc cations into [B]-ZSM-5 (table 3.3). In this case, however, the yield of alkanes remains low. This is because the aromatics are formed by   the direct dehydrogenation of olefins by the action of zinc species. As exemplified by this case, it is possible to achieve catalysis by metal cations at the same time suppressing catalysis by acid.

The acid strength of [Fe]-ZSM-5 can be inferred to be weak from the very low yield of alkanes and aromatics in the conversion of methanol of olefins. Holderich reported that ketone can be isomerized to aldehyde in a high over [B]-ZSM-5. ZSM-5 gave only low selectivity.

R1R2R3CCHO $\longrightarrow$ R1R2CHCR
$\parallel$
O
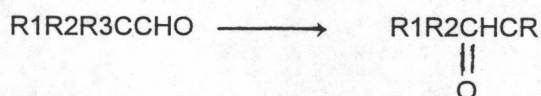
Since the acidic strength of [B]-ZSM-5 is weak, the role of the trace amount of aluminum   impurity   may not be negligible in their catalysts. Chu et al. examined the catalytic activities of [B]-ZSM-5 containing varying   amounts of framework B for a number of
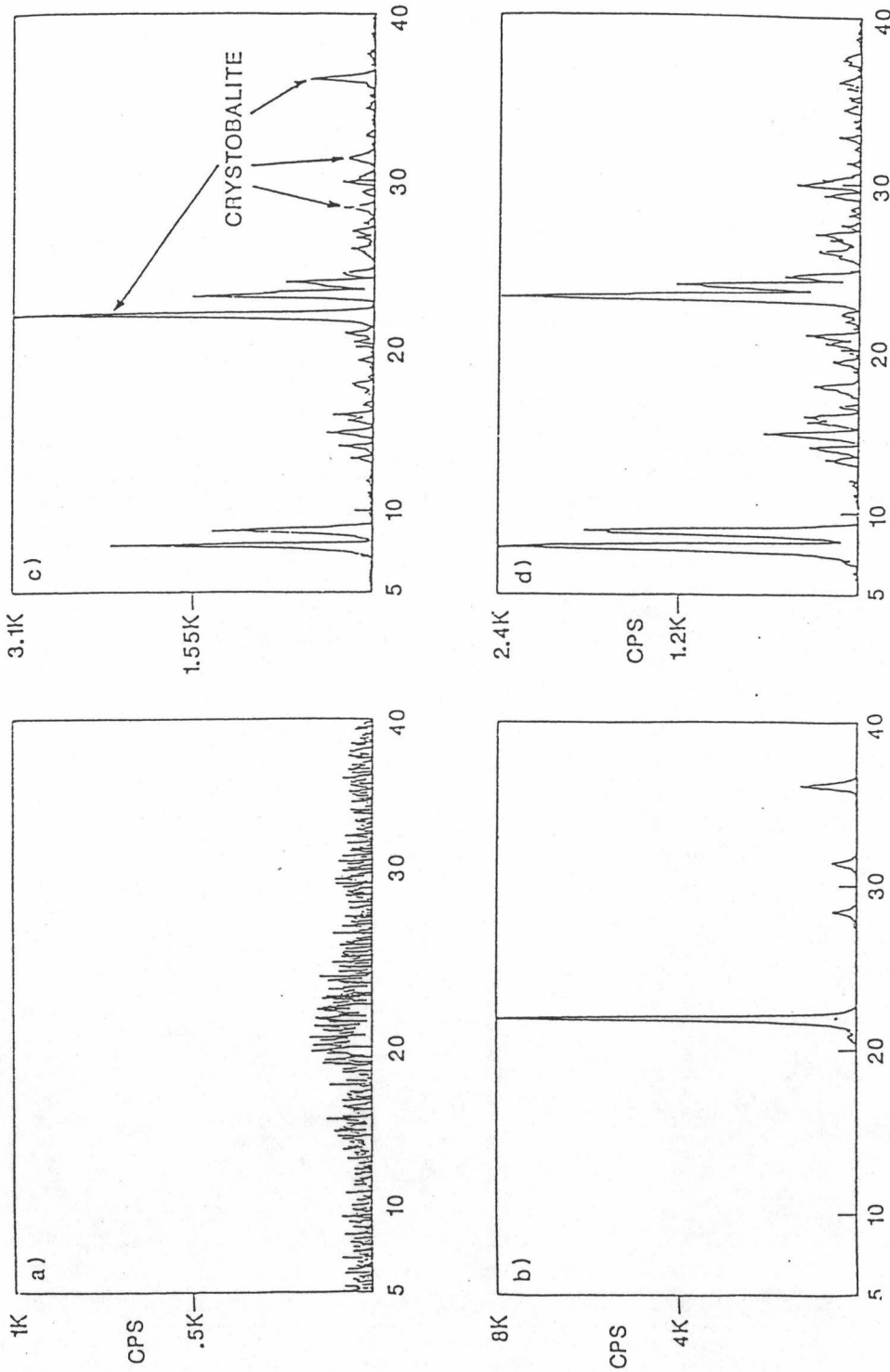
Figure 3.16 X-ray powder diffraction used to identify phases in synthesis of zeolites [66].

a) Noncrystalline product

b) crystalline but non-zeolitic phase (cristobalite shown in this example)

c) mixture of phase (crystobalite and ZSM-5)   d) pure single crystalline phase(ZSM-5)

acid-catalyzed reactions and concluded that the catalytic activity was due, if not entirely, to trace amounts (80-580 ppm) of framework aluminum [67].

3.7 X-ray Powder Diffraction

3.7.1 Identification of Crystalline Material

The first step in characterization of the solid isolated from the synthesis mixture is X-ray powder diffraction. The most significant information obtained about the solid is obtained from the diffraction pattern. This includes :

1. Successful (or unsuccessful) formation of a crystalline material.
2. Presence of a single phase or mixture of phases.
3. With the presence of sufficient peaks, the identification of the structure type or structure types comprising the mixture.
4. If standards are available, the level of crystallinity obtained from that synthesis batch.
5. Ultimately, with the proper techniques, determination of a new structure.

The X-ray powder diffraction pattern of the solid obtained from the zeolite synthesis mixture is generally taken between the values of 5 °2θ and 40 °2θ . It is within this range that the most intense peaks characteristic of the zeolite structure occur. The peaks at values higher than 40 °2θ are of significantly low intensity, and, depending on the level of crystallinity, may not be observable. Therefore, for most routine X-ray identification of zeolite phases, the range between 5 and 40 ° 2θ is examined.

A common occurrence in zeolite synthesis is the presence of a noncrystalline product from a given reaction mixture. An example of an X-ray diffraction pattern for a

typical unsuccessful synthesis is shown in figure 3.16(a). Beside the noncrystalline products possible form a give reactive mixture, crystalline but non-zeolite material may be obtained. The commonly observed crystalline phase obtained from an unsuccessful synthesis of the high-silica zeolites, for example, is cristobalite, a dense quartz phase. The cristobalite phase is a simple pattern to recognize, as it contains only one very intense line, between 5° 2θ and 40° 2θ. A typical X-ray trace of cristobalite is shown in figure 3.16(b). In some systems, mixtures are obtained. These can be readily identified if individual X-ray diffraction patterns of both components are already known. For example, in figure 3.16(c), a mixture of cristobalite and ZSM-5 was produced from the reaction mixture. As both components are already well known, a comparison of these values with standard literature values for the X-ray diffraction patterns of cristobalite and ZSM-5 will confirm these components of the mixture. By changing the synthesis parameters, the zeolite phase can (in many cases) be optimized and the second phase suppressed, as shown in figure 3.16(d).Here a sharp pattern for a well-crystallized ZSM-5 sample was obtained.

Many times in exploratory zeolite synthesis aimed at producing new structures, material are obtained with X-ray patterns that appear to indicate a single phase and are already related in peak position to a known structure. However, in some cases the peak intensities are not in agreement. Changes in relative peak intensity have been to occur :

1. Upon removal of an organic additive from the pores or changing the cations within the pores of the higher-silica-contain materials.
2. Upon changing the counter-ion.
3. When large crystals have a preferred orientation in the X-ray sample holder.
4. When other ions are substitute into the framework structure.

It is important to consider any features that may arise when comparing X-ray diffraction patterns of one's material with those patterns reported in the literature. Two such

effects are illustrated in figures 3.17 and 3.18 [1], and the effect the presence of the organic moiety contained within the pores of a high-silica material has on the intensity of the X-ray diffraction peaks is shown in figure 3.19 for the ZSM-5 system. In figure 3.17, X-ray powder diffraction patterns were obtained from zeolite ZSM-5 crystallized under two different reaction mixture conditions. The diffraction pattern shown in figure 3.17 (a) was obtained from a material has been crystallized from TPA/NH4/K system and produced the diffraction typical of the ZSM-5 structure. In figure 3.17 (b), the diffraction pattern arises from the material crystallized from the TPA/NH4/Li system This material is highly crystalline, composed of large coffin-shaped, nearly single, crystals characteristic of ZSM-5. However, because of the large and regular size of the crystals, the crystals tended to pack in the X-ray sample holder in a prefered orientation, causing the observed drastic change in diffraction pattern peak intensity. The peak near 7.9 º 2θ decreases dramatically in intensity, while the peak near 8.9 º 2θ becomes the most intense line in the diffraction pattern.
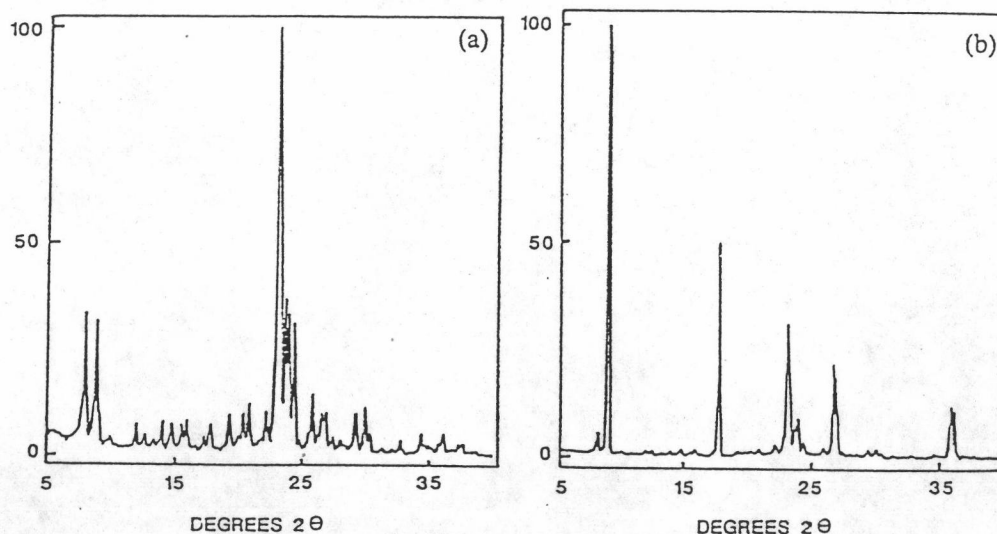

Figure 3.17 (a) X-ray diffraction pattern of ZSM-5 produced with 1.5 K_2O ;

(b) X-ray diffraction pattern of ZSM-5 produced in system with

1.0 Li_2O. The difference in intensies between the two diffraction

patterns is due to preferred orientation of the larger ZSM-5

crystal obtained from lithium system [66].

Synthesis of nonaluminosillcate molecular sieves with zeolite structures will sometimes give rise to diffraction patterns that differ in intensity. figure 3.18 shows three patterns for the molecular sieve: iron silicate, gallium sillicate, and aluminum silicate with the sodalite structure. All three materials were prepared under similar conditions with SiO_2/M_2O_3 ratios around 10. Though all three are the sodalite structure, the line intensities vary with differing M (M = Fe, Ga, or Al). The X-ray liner at 28 º 2 θ is present in the iron and gallium silicate and absent in the aluminum, whereas the line at 38 º 2θ is absent in the ferrisilicate and present to varying degree in the gallium and aluminum silicate systems.

Changes may also take place in the X-ray diffraction peak intensities when the zeolite is thermally treated to remove the organic crystal-directing agent. Such changes observed for the ZSM-5 system are shown in figure 3.19, and are characteristic of the changes observed in the X-ray diffraction pattern of thermally treated ZSM-5 regardless of SiO_2/Al_2O_3. Similar observations have been make for the ferrisilicate analogs as well. The central peaks between 2θ of 22 and 24° reduced marginally during the thermal. However, this decrease is accompanied by increases in the intensities of the two peaks at 2θ of 7.9 and 8.9 ^{O}. Little relative change was observed for the other peaks. Minimal changes normally are observed in the X-ray diffraction pattern of this material after further thermal or hydrothermal treatment.

Reporting the peak intensities of an X-ray diffraction pattern for a given structure that exhibits such variability in peak intensity is generally done by indicating a range in intensity for a given peak. An example of this is shown in table 3.4, which is taken from the patent literature.
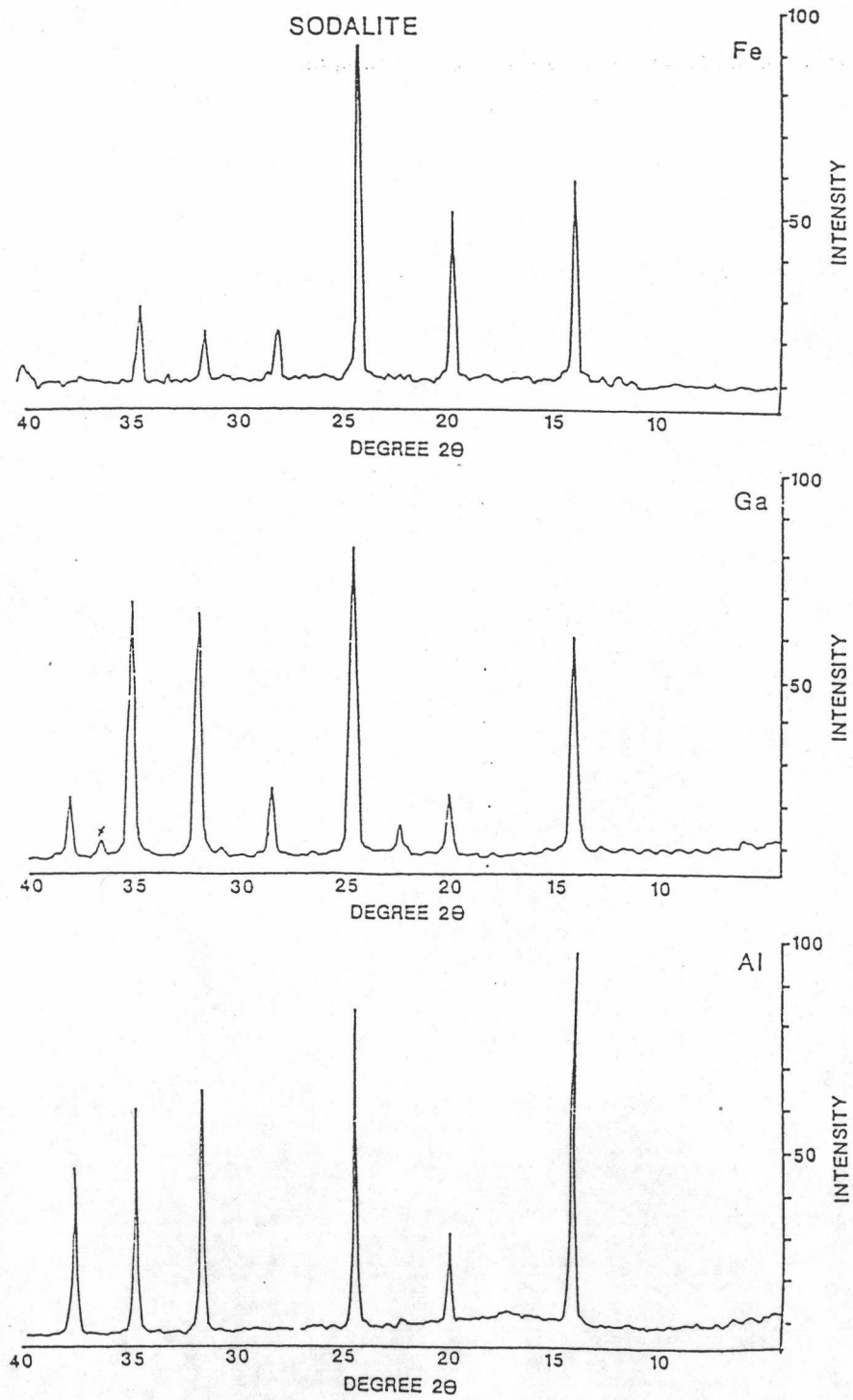
Figure 3.18 Changes in intensity of X-ray diffraction peaks with changing elemental composition in the sodalite structure. The comparison is between framework substituted iron (top), gallium (center), and the analogous aluminum (bottom). SiO_2/M_2O_3 (M=Al, Ga, or Fe) ca. 10 [66].
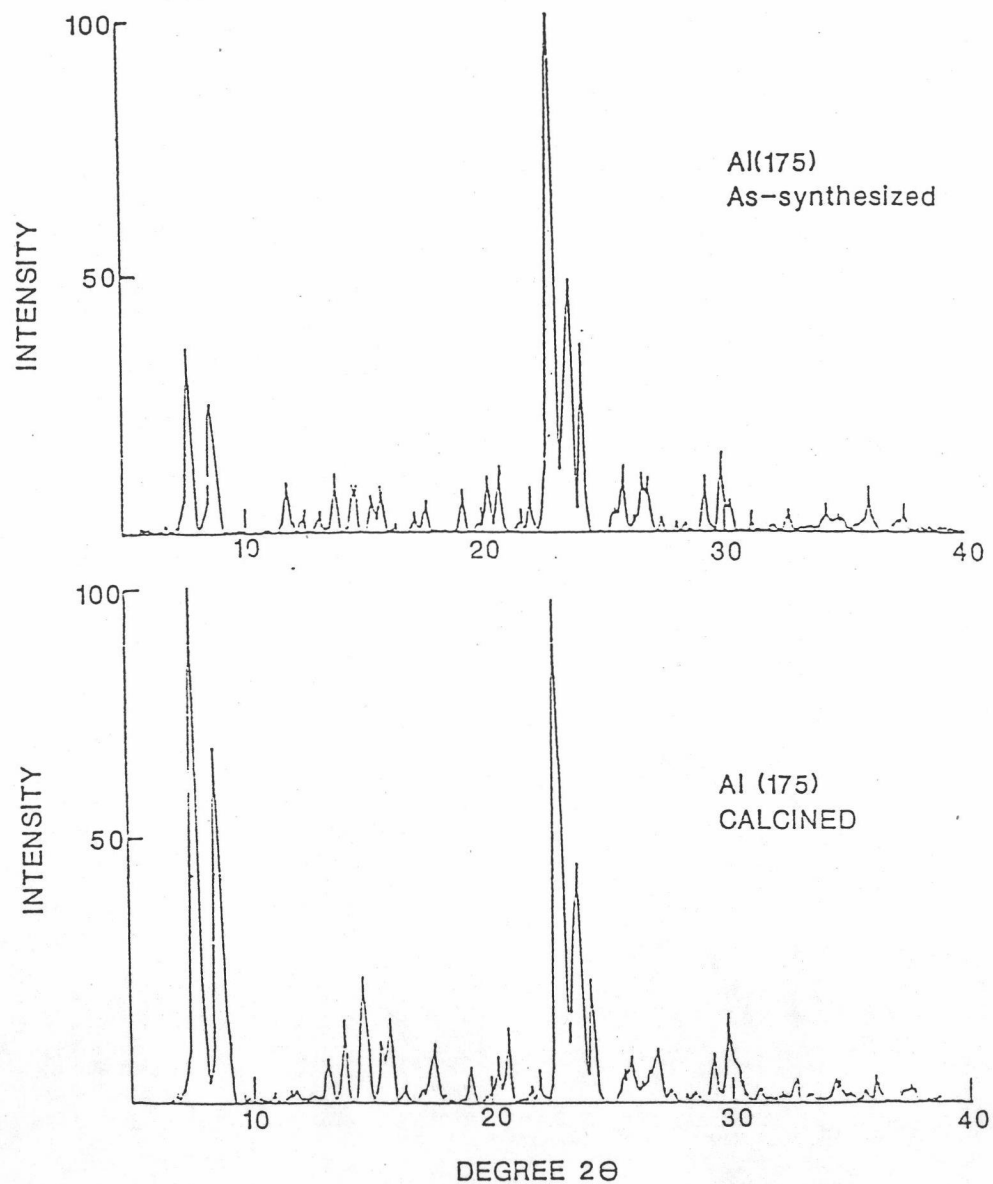
Figure 3.19 Changes in intensity of X-ray diffraction peaks with removal of the organic quaternary amine crystal-directing agent in the ZSM-5 system [66].

Table 3.4 An example of reporting variable peak intensities found in the X-ray powder diffraction patterns for crystals with the EU-4 structure (EP0063436) [66].

d (Å)	I	d (Å)	I
11.1	vs	3.98	vs
9.2	w-vs	3.69	s
4.621	vs	3.58	s
4.46	w-s	3.34	s
4.28	vs	3.26	s-vs

Table 3.5 Reflections that have been used to determined crystallinity in the faujasite materials [66].

2θ	hkl	2θ	hkl
15.4	331	25.6	624
18.4	333	30.8	660
20.1	440	31.4	555
23.3	533	34.4	664

3.7.2 Measuring X-ray Crystallinity

A quantitative measure of the crystallinity of a zeolite is made by using the summed heights of approximately eight peaks in the X-ray diffraction pattern. The peaks chosen are selected specifically because they are least affected by degree of hydration of the sample and minimally affected by other factors, for the faujasite materials, the eight reflections generally chosen are listed in table 3.5 [66]. In the zeolite ZSM-5 system, on the other hand, four lines corresponding to a 2θ range of 22.5 to 24 $^{\circ}$ have been used with relative success.

The percent crystallinity is taken as the sum of the peak heights of the unknown material divided by the sum of the peak heights of a standard faujasite material that has been designated to be 100 % crystalline:

$$\% \text{ cryst.} = \frac{\text{Sum of peak heights (unknown)}}{\text{Sum of peak heights (standard)}}$$

In general, peak heights can be successfully used in measuring X-ray crystallinity provided that the crystals being examined are larger than 0.3 micron. Below this value, in the faujasite system, broadening of the X-ray lines is observed due to small crystal size effects.

Peak areas also can be examined. In the faujasite system, the area of the peak at 26.6 has been used to calculate crystallinity. The area of the peak at 26.6 for the unknown material divided by the area of that peak for a known, 100% crystalline material provides information on the percent crystallinity of any given faujasite sample [66]:

$$\% \text{ cryst.} = \frac{\text{Area(unknown)}}{\text{Area(standard)}}$$

3.8 Acidity Measurements from Ammonia Desorption

Temperature programmed desorption (TPD) of ammonia is commonly used to measure both acid site concentration and strength. Semiquantitative data about the concentration of acid sites in the material are obtained from gravimetric or volumetric techniques. Quantitative information requires identification of ammonia via continuous mass spectrometry, titration, or infrared monitoring. The titration method of Kerr is the most reliable as all of the ammonia is quantitatively measured. There are two methods of preparing the samples for examination by TPD: (a) ion exchange to obtain the NH_4^+ form and (b) adsorption of ammonia gas on the acid form of the zeolite or molecular sieve. Difficulties in the latter method arise from physisorption of excess ammonia.

A simple method of quickly screening the zeolites and other molecular sieves for their acid strength has involved monitoring the loss of ammonia with increasing temperature. The temperature at which most of the ammonnia (in the form of NH_4^+) is no longer retained within the material has been related to the acid strength of that material. The desorption peak maximum, however, is related to the rate at which the sample is heated. Thus the TPD of the adsorbed base is a kinetic phenomenon and not an equilibrium phenomenon, and the peak maximum, T_M, can be related to the heating rate, B, through:

$$2 \log T_M - \log B = \frac{E_d}{2.3RT_M} + \log \frac{E_d \cdot a_m}{Rk_o}$$

where a_m is the amount adsorbed at saturation, k_o is the exponential factor in the desorption rate, and E_d is the activation energy for desorption. This equation assumes that no readsorption occurs, and that the adsorption sites are sufficiently distant form one another to preclude any mutual interactions.

Comparative studies of the acid strength of several materials will provide information on trends observed from ammonia TPD. More rigorous identification of acid sites in the zeolites and other molecular sieves generally has involved two or more techniques. A common set of techniques includes TPD and infrared spectroscopy. A combination of TPD and NMR also has been used [66].

3.9 Ion-exchange Reaction in Zeolites

The cation exchange property of zeolite minerals was first observed 100 years ago. The ease of cation exchange in zeolites and other minerals led to an early interest in ion exchange materials for use as water softening agents. Synthetic, noncrystalline aluminosilicate materials were primarily used; in more recent years, organic ion exchange resins are used, Crystalline zeolites have not been used commercially as water softeners.

The ion exchange behaviour of various inorganic exchangers and other types of crystalline silicates such as clay minerals and feldspathoids has been extensively reviewed. Because of their three-dimensional framework structure, most zeolites and feldspathouds do not undergo any appreciable dimensional change with ion exchange; clay minerals, because of their two-dimensional structure, may undergo swelling or shrinking with cation exchange. One application for commonly occurring zeolite minerals (such as clinoptilolite) is in the selective removal of radioactive ions from radioactive waste materials.

The cation exchange behaviour of zeolites depends upon (1) the nature of the cation species, the cation size, both anhydrous and hydrated, and cation charge; (2) the temperature; (3) the concentration of the cation species in solution ;(4) the anion species associated with the cation in solution; (5) the solvent(most exchange has been carried out in aqueous solutions, although some work has been done in organic solvents); and (6) the structural characteristics of the particular zeolite. Cation selectivities in zeolites do not follow the typical rules that are evidenced by other inorganic and organic exchangers. Zeolite structures have unique features that lead to unusual types of cation selectively and sieving. The recent structural analyses of zeolites form a basis for interpreting the variable cation exchange behaviour of zeolites.

Cation exchange in zeolite is accompanied by dramatic alteration of stability, adsorption behaviour and selectivity, catalytic activity and other important physical properties. Since many of these properties depend upon controlled cation exchange with particular cation species, detailed information on the cation exchange equilibria is important. Extensive studies of the ion exchange processes in some of the more important mineral and synthetic zeolites have been conducted [75].

3.10 Oxide of Nitrogen

The known oxides of nitrogen are listed in table 3.6 [76], and their structures are shown in figure 3.20 [76].

3.10.1 Nitrous Oxide.

Nitrous oxide (N_2O) is obtained by thermal decomposition of ammonium nitrate in the melt at 250° to 260° :
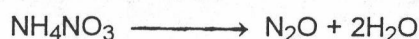
$$NH_4NO_3 \longrightarrow N_2O + 2H_2O$$

Table 3.6 Oxides of nitrogen [76].

Oxides of Nitrogen

Formula	Name	Color	Temperatures (°C)	Remarks
N_2O	Nitrous oxide	Colorless	m. −90.8; b. −88.5	Rather unreactive
NO	Nitric oxide	Colorless	m. −163.6; b. −151.8	Moderately reactive
N_2O_3	Dinitrogen trioxide	Dark blue	f.p. −100.6; d. 3.5	Extensively dissociated as gas
NO_2	Nitrogen dioxide	Brown	m. −11.20	Rather reactive
N_2O_4	Dinitrogen tetroxide	Colorless	b. 21.2	Extensively dissociated to NO_2 as gas and partly as liquid
N_2O_5	Dinitrogen pentoxide	Colorless	m. 30; d. 47	Unstable as gas; ionic solid
NO_3; N_2O_6	—	—		Not well characterized and quite unstable

[18] G. Bengtsson. *Acta Chem. Scand.*, 1973, 27, 1717.
[19] R. Kummel and F. Pieschel. *Z. Anorg. Allg. Chem.*, 1973, 396, 90.
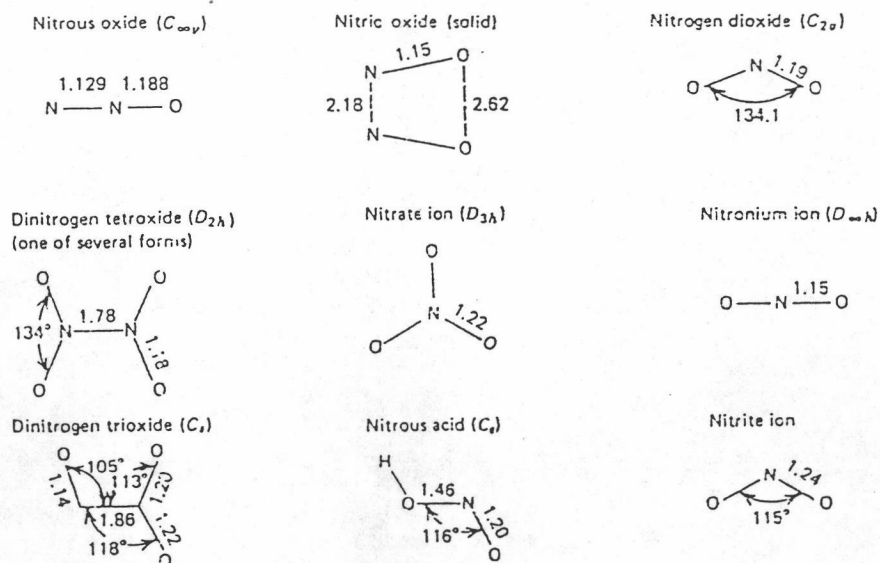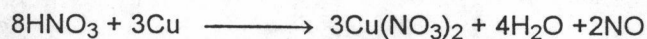

Figure 3.20 The structures and point group symmetries of some nitrogen oxides and anions [76] (angles in degrees; bond lengths in A).

The contaminants are NO, which can be removed by passage through iron (II) sulfate solution and 1 to 2% of nitrogen. The NH_4NO_3 must be free from Cl^-, since this catalytically causes decomposition to N_2. However heating HNO_3 or H_2SO_4 solutions of NH_4NO_3 with small amounts of Cl^- gives almost pure N_2O. The gas is also produces in the reduction of nitrites and nitrates under certain conditions and by decomposition of hyponitrites.
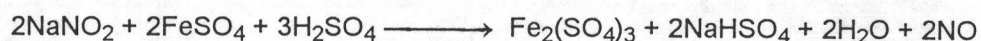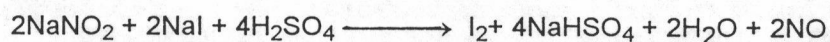
Nitrous oxide is relatively unreactive, being inert to the halogens, alkali metals, and ozone at room temperature. It will oxidize some low-valent transition metal complexes and forms the complex $[Ru(NH_3)_5 N_2O]^{2+}$. At elevated temperatures it decomposes to nitrogen and oxygen, reacts with alkali metals and many organic compounds, and supports combustion. Apart from its anesthetic role, its chief commercial use is as an aerosol propellant.
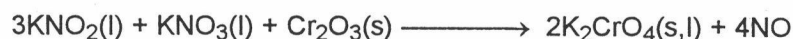
3.10.2 Nitric Oxide

Nitric oxide (NO) is formed in many reactions involving reaction of nitric acid and solutions of nitrates and nitrites. For example, with 8M nitric acid:

$$8HNO_3 + 3Cu \longrightarrow 3Cu(NO_3)_2 + 4H_2O + 2NO$$

Reasonably pure NO is obtained by the following aqueous reactions:

$$2NaNO_2 + 2NaI + 4H_2SO_4 \longrightarrow I_2 + 4NaHSO_4 + 2H_2O + 2NO$$

$$2NaNO_2 + 2FeSO_4 + 3H_2SO_4 \longrightarrow Fe_2(SO_4)_3 + 2NaHSO_4 + 2H_2O + 2NO$$

or dry:

$$3KNO_2(l) + KNO_3(l) + Cr_2O_3(s) \longrightarrow 2K_2CrO_4(s,l) + 4NO$$

Commercially it is obtained by catalytic oxidation of ammonia as already noted. Direct combination of the elements occurs only at very high temperatures, and to isolate the small amounts so formed (a few volume percent at 300 °C) the equilibrium must be rapidly chilled. Though much studied, this reaction has not been developed into a practical commercial synthesis.

Nitric oxide reacted instantly with O_2 :

$$2NO + O_2 \longrightarrow 2NO_2$$
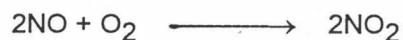
It also reacts with F_2, Cl_2 and Br_2 to form the nitrosyl halides XNO and with CF_3I to give CF_3NO and I_2. It is oxidized to nitric acid by several strong oxidizing agents; the reaction with permanganate is quantitative and provides a method of analysis. It is reduced to N_2O by SO_2 and to NH_4OH by chromium (II) ion, in acid solution in both cases.

Nitric oxide as thermodynamically unstable at 25 °C and 1 atm and at high pressures it readily decomposes in the range 30-50 °C :

$$3NO \longrightarrow N_2O + NO_2$$

The NO molecule has the electron configuration $(\sigma 1)^2(\sigma 1^*)^2(\sigma 2, \pi)^6(\pi^*)$. The unpaired $\pi*$ electron renders the molecule paramagnetic and partly cancels the effect of the - bonding electrons. Thus the bond order is 2.5, consistent with an interatomic distance of 1.15 Å, which is intermediate between the triple-bond distance in NO^+ (see below) of 1.06 Å and representative double-bond distances of ~1.20 Å.

Nitric oxide dimerizes in the solid state and dimers also persist in the vapor at the boiling point. The binding energy of the dimer is less than 10 kJ mol $^{-1}$, consistent with the long N-N bond. The dimer has no unpaired spins but feeble intrinsic temperature-independent paramagnetism. Unstable forms can be isolated in matrices.

The electron in the $\pi*$ orbital is relatively easily lost (ΔH_{ion} = 891 kJ mol^{-1}), to give the *nitrosonium ion* NO$^+$, which has an extensive and important chemistry. Because the electron removed comes out of an antibonding orbital, the bond is stronger in NO$^+$ than in NO$^-$: the bond length decreases by 0.09 $\overset{o}{A}$ and the vibration frequency rises from 1840 cm^{-1} in NO to 2150-2400 cm^{-1} (depending on environment) in NO$^+$. Numerous ionic compounds of NO$^+$ are known.

When N_2O_3 or N_2O_4 is dissolved in concentrated sulfuric acid , the ion is formed:

$$N_2O + 3H_2SO_4 = 2NO^+ + 3HSO_4^- + H_3O^+$$

$$N_2O_4 + 3H_2SO_4 = NO^+ + NO_2^+ + 3HSO_4^- + H_3O^+$$
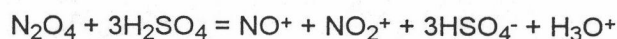
The isolable compound NO$^+$HSO$_4^-$, nitrosonium hydrogen sulfate, is an important intermediate in the lead-chamber process for manufacture of sulfuric acid. Its saltlike constitution has been shown by electrolysis, conductivity studies, and cryoscopic measurements. The compounds NO$^+$ClO$_4^-$ and NO$^+$BF$_4^-$, both isostructural with the corresponding ammonium and H$_3$O$^+$ compounds, are known; many others such as (NO)$_2$ PtCl$_6$, NOFeCl$_4$, NOAsF$_6$, NOSbF$_6$, and NOSbCl$_6$ may be made in the following general way:
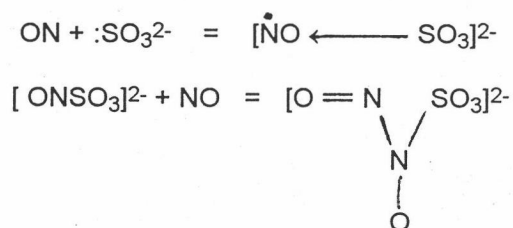
$$NO + MoF_6 \longrightarrow NO^+MoF_6^-$$

$$ClNO + SbCl_5 \longrightarrow NO^+SbCl_6^-$$
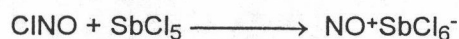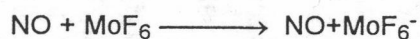
All such salts are readily hydrolyzed :

$$NO^+ + H_2O \longrightarrow H^+ + HNO_2$$

and they must be prepared and handled under anhydrous conditions.

In alkaline solution at 0 ºC , SO_3^{2-} reacts with NO to give a white crystalline solid, potassium *N*-nitrosohydroxylamine-*N*-sulfonate ($K_2SO_3N_2O_2$) :

$$ON + :SO_3^{2-} \quad = \quad [\overset{\bullet}{N}O \longleftarrow SO_3]^{2-}$$

$$[ONSO_3]^{2-} + NO \quad = \quad [O = N \quad SO_3]^{2-}$$

Other species with N_2O_2 groups are obtained by interaction of amines with NO; alcohol in base also gives $[O_2N_2CH_2N_2O_2]^{2-}$.

The NO^+ ion is isoelectronic with CO, and, like CO, will form bonds to metals. Thus, for example, analogous to nickel carbonyl, $Ni(CO)_4$, there is the isoelectronic $Co(CO)_3NO$.

3.10.3 Dinitrogen Trioxide.

This oxide is best obtained by interaction of stoichiometric quantities of NO and O_2 or NO and N_2O_4 as an intensely blue liquid and a pale blue solid. It is formally the anhydride of nitrous acic and dissociation of and equimolar mixture of NO and NO_2 in alkalis gives virtually pure nitrite; in the gas phase nitrous acid is formed.

The dissociation of N_2O_3 :

$$N_2O_3 = NO + NO_2$$

begins to be significant above -30 $^\circ$C. There appears to be some self-ionization in the liquid;

$$N_2O_3 \rightleftharpoons NO^+ + NO_2^-$$

The molecule is polar in the sense $ON^{\delta+}$ ——— $NO_2^{\delta-}$. The stable structure in the solid has along N———N bond, and this structure persists in the liquid and gas (figure 3.20).

3.10.4 Nitrogen Dioxide and Dinitrogen Tetroxide.

These two oxides, NO_2 and N_2O_4, exist in a strongly temperature-dependent equilibrium

$$2NO_2 \rightleftharpoons N_2O_4$$

(Brown paramagnetic)   (Colorless diamagnetic)
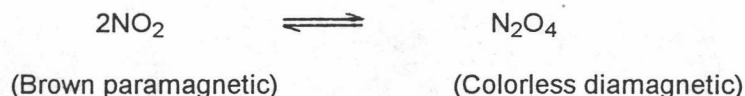
both in solution and in the gas phase, where ΔH^o_{298} for dissociation is 57 kJ mol-1. In the solid state the oxide is wholly N_2O_4. Partial dissociation occurs in the liquid; it is pale yellow at the freezing point and contained 0.01% of NO_2, which increases to 0.1% in the deep red-brown liquid at the boiling point, 21.15$\circ$C . In the vapor at 100 $^\circ$C the composition is NO_2 90%,N_2O_4 10%, and dissociation is complete above 140 $\circ$C. Molecular beam mas spectrometric studies indicate that trimers and tetramers occur, but there is no evidence for such species under normal conditions.

The monomer NO_2 has an unpaired electron and its properties, red-brown color and ready dimerization to colorless and diamagnetic N_2O_4, are not unexpected for such a radical.
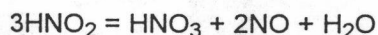
NO_2 can also lose its odd electron fairly readily (ΔH_{ion} = 928 kJ mol-1) to give NO_2^+, the nitronium ion, discussed below.

Although other forms can exist inert matrixes the most stable form of N_2O_4 is that shown in figure 3.20. This molecule has unusual features : namely, the planarity and the long N——N bond, 1.78 $\overset{o}{A}$ compared to 1.47 in H_2N——NH_2. Molecular orbital calculations suggest that although the long N——N bond is of σ type, it is long because of delocalization of the electron pair over the whole molecule, with large repulsion between doubly occupied MOs of NO_2. The coplanarity results from a delicate balance of forces favoring the skew and planar forms. The barrier to rotation about the N——N bond is estimated to be about 9.6 kJ mol^{-1}.

The mixed oxides are obtained by heating metal nitrates, by oxidation of nitric oxide in air, and by reduction of nitric acid and nitrates by metals and other reducing agents. The gases are highly toxic and attack metals rapidly. They react with water:

$$2NO_2 + H_2O = HNO_3 + HNO_2$$
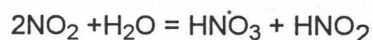
the nitrous acid decomposing, particular when warmed:

$$3HNO_2 = HNO_3 + 2NO + H_2O$$

The thermal decomposition

$$2NO \rightleftharpoons 2NO + O_2$$

begins at 150 °C and is complete at 600 °C.

The oxides are fairly strong oxidizing agents in aqueous solution, comparable in strength to bromine:

$$N_2O_4 + 2H^+ + 2e = 2HNO_2 \quad E^0 = +1.07 \text{ V}$$

The mixed oxides, "nitrous fumes," are used in organic chemistry as selective oxidizing agents; the first step is hydrogen abstraction:

$$RH + NO_2 = R \cdot + HONO$$
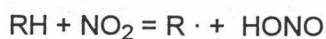
and the strength of the C———H bond generally determines the nature of the reaction.

Nitrogen dioxide and nitric oxide, commonly referred to as NO_x, are both of concern in atmospheric pollution being produced in combustion.

Dinitrogen tetroxide has been extensively studied as a nonaqueous solvent. The electrical conductivity of the liquid is quite low, and self-ionization is very endothermic.

$$N_2O_4 \rightleftharpoons NO^+ + NO_3^- \quad \Delta H = 49.8 \text{ kJ mol}^{-1}$$
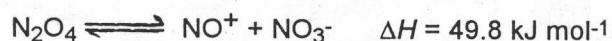
It forms molecular addition compounds with a great variety of nitrogen, oxygen, and aromatic donor compounds. Systems involving liquid N_2O_4 mixed with an organic solvent are often very reactive; for example, they dissolve relatively noble metals to form nitrates, often solvated with N_2O_4. Thus copper reacts vigorously with N_2O_4 in ethyl acetate to give crystalline $Cu(NO_3)_2 \cdot N_2O_4$, from which anhydrous, volatile (at 150° - 200°C) cupric nitrate is obtained. Some of the compounds obtained in this way may be formulated as nitrosonium salts, for example, $Zn(NO_3)_2 \cdot 2N_2O_4$ as $(NO^+)_2[Zn(NO_3)_4]^{2-}$.

X-ray diffraction studies of $Cu(NO_3)_2 \cdot N_2O_4$ confirm that no molecular N_2O_4 is present; it consists of NO^+ ions and polymeric nitrato anions The complex $Fe(NO_3)_3(1.5 \ N_2O_4)$ also appears to have a nitrato anion $[Fe(NO_3)_4]^-$, but with a cation $N_4O_6^{2+}$ that can be regarded as NO_3^- bound to three NO^+ groups.

In anhydrous acids N_2O_4 dissociates ionically, as in H_2SO4 above, and in anhydrous HNO3 dissociation is almost complete:

$$N_2O_4 = NO+ + NO_3^-$$

The dissociation in H_2SO_4 is complete in dilute solution; at higher concentrations undissociated N_2O_4 is present, and at very high concentrations nitric acid is formed :

$$N_2O_4 + 3H_2SO_4 = NO^+HSO_4^- + HNO_3 + HSO_4^- + SO_3 + H_3O^+$$
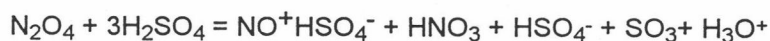
The $NOHSO_4$ actually crystallizes out. The detailed mechanism and intermediates are undoubtedly complex.

3.10.5 Dinitrogen Pentoxide.

The oxide N_2O_5 is usually obtained by dehydration of nitric acid with P_2O_5: it is not too stable (sometimes exploding) and is distilled in a current of ozonized oxygen.
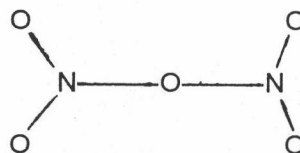
$$2HNO_3 + P_2O_5 \longrightarrow 2HPO_3 + N_2O_5$$

It is, conversely, the anhydride of nitric acid:

$$N_2O_5 + H_2O \longrightarrow 2HNO_3$$

It is deliquescent, readily producing nitric acid by the reaction above.

The gaseous compound appears to have a structure of type

with a bent N——O——N group, although this angle may be near 180 $^\circ$. Solid N_2O_5 in its stable form is nitronium nitrate ($NO_2^+NO_3^-$), but when the gas is condensed on a surface at ~ 90° K, the molecular form is obtained and persists for several hours. On warming to ~200° K, however, the latter rapidly changes to $NO_2^+NO_3^-$. The structures of the two ions are shown in figure 3.20 .

As with N_2O_4, ionic dissociation occurs in anhydrous H_2SO_4, HNO_3, or H_3PO_4 to produce NO_2, for instance,

$$N_2O_5 + 3H_2SO_4 \rightleftharpoons 2NO_2^+ + 3H_2SO_4^- + H3O^+$$

Many gas phase reactions of N_2O_5 depend on dissociation to NO_2 and NO_3, with latter then reacting further as an oxidizing agent. These reactions are among the better understood complex inorganic reactions.

In the N_2O_5-catalyzed decomposition of ozone, the steady state concentration of NO_3 can be high enough to allow its absorption spectrum to be recorded [76].